Food Chemistry 186 (2015) 292–297

Contents lists available at ScienceDirect

Food Chemistry

journal homepage: www.elsevier.com/locate/foodchem

Interaction between Z-ligustilide from *Radix Angelica sinensis* and human serum albumin

Tingting Chen *, Xiting Zhu, Qi Chen, Ming Ge, Xueping Jia, Xiang Wang, Cunwang Ge *

School of Chemistry and Chemical Engineering, Nantong University, Nantong 226019, PR China

ARTICLE INFO

Article history:
Available online 14 November 2014

Keywords:
Human serum albumin
Z-ligustilide
Interaction
Fluorescence
Circular dichroism

ABSTRACT

Z-ligustilide (LIG), an essential oil extract from *Radix Angelica sinensis*, has broad pharmaceutical applications in treating cardiovascular and cerebrovascular diseases. Interaction of LIG with the major transport protein of human blood circulation, human serum albumin (HSA) has been investigated by steady-state, UV–vis and circular dichroism (CD) spectroscopic methods, as well as the effect of metal ions (e.g. Zn^{2+}, Cu^{2+}, Fe^{3+}, Co^{2+}, Ni^{2+}) on the LIG–HSA system. Fluorescence results revealed that a moderate binding affinity ($1.59 \times 10^4\ M^{-1}$ at 298 K) between LIG and HSA with a 1:1 stoichiometry. Thermodynamic analysis of the binding data ($\Delta S = +12.96\ J\ mol^{-1}\ K^{-1}$ and $\Delta H = -20.11\ kJ\ mol^{-1}$) suggested the involvement of hydrophobic and van der Waals forces, as well as hydrogen bonding in the complex formation. The specific binding distance r (3.75 nm) between donor (Trp-214) and acceptor (LIG) was obtained according to fluorescence resonance energy transfer. CD results showed that slight conformational changes occurred in the protein upon complexation with LIG.

1. Introduction

Danggui, known as *Radix Angelica sinensis* (RAS) has been considered a medicinal plant and applied to alleviated various disease syndromes in traditional Chinese medicine. Z-ligustilide (LIG) (Inset in Fig. 1) is one of the most active components of the essential oils of RAS (Zhao, Jiang, Wu, Cao, & Gao, 2014). LIG displays a variety of pharmacological and biological activities. It can reduce vascular resistance; thereafter, increase blood flow and enhance microcirculation to prevent cardiovascular disease, including atherosclerosis and hypertension. LIG is also known to have a protective effect against ischemic brain injury caused by the failure of regular blood supply to local brain tissue in the central nervous system (CNS) (Yin et al., 2013). LIG can decrease the level of malondialdehyde, a product of lipid peroxidation, and increase the activity of antioxidant enzymes, fostering an anti-apoptotic effect that reduces cerebral infarct volumes and improves neurobehavioral deficits (Kuang et al., 2006).

Human serum albumin (HSA) is the most abundant protein in blood plasma, accounting for about 60% of the total protein amount, which corresponds to a concentration of 42 g/L. It is a globular protein consisting of 585 amino acid residues and has three homologous domains (I–III). Each domain comprises two subdomains (A and B) and is stabilized by 17 disulfide bridges (Sugio, Kashima, Mochizuki, Noda, & Kobayashi, 1999). HSA has one tryptophan residue, Trp214, located in subdomain IIA (He & Carter, 1992). The principal regions of ligand binding to HSA are located in hydrophobic cavities in subdomains IIA and IIA, which are consistent with Sublow site I and II, respectively (Sudlow, Birkett, & Wade, 1975). These binding sites underline the exceptional ability of HSA to interact with many organic and inorganic molecules, thereby making this protein an important regulator of the pharmacokinetic behaviour of many drugs as well as intercellular fluxes (Varshney, Rehan, Subbarao, Rabbani, & Khan, 2011). HSA binding of a bioactive compound leads to improved solubility in plasma, reduced toxicity, protection against oxidation, as well as prolonged *in vivo* half-life of the bound molecule (Xiao & Kai, 2012; Xiao, 2013). Upon absorption exogenous substances like drugs enter into the circulatory system and bind reversibly to serum albumin. The degree of affinity between serum albumin and the drug can govern the distribution of the drug into tissues, affect the elimination of the drug and consequently affect the therapeutic or toxic effects of the drug (Ghuman et al., 2005). Therefore, it is significant to investigate the drug-HSA interaction for deeply understanding the pharmacodynamics and pharmacokinetics behaviour of drugs. The topic has become an important research field in life sciences, chemistry, and clinical medicine.

Despite the publication of many reports illustrating the various pharmacological properties of LIG, a comprehensive study in its interaction with the major transport protein of the human blood

* Corresponding authors. Tel.: +86 513 85012851 (T. Chen), +86 513 85012853 (C. Ge).
E-mail addresses: ttchen1980@126.com (T. Chen), cuwangge@126.com (C. Ge).

http://dx.doi.org/10.1016/j.foodchem.2014.11.041
0308-8146/

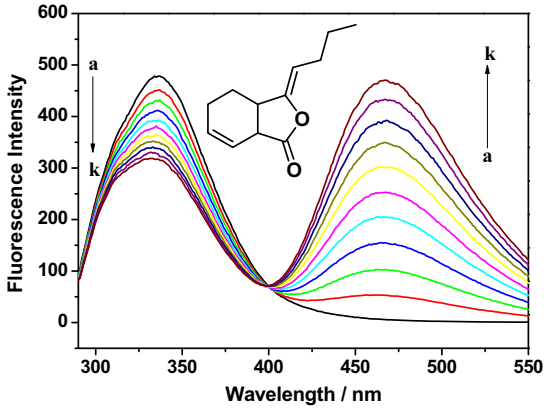

Fig. 1. Effect of LIG on fluorescence spectra of HSA. (a) 3.0 μM HSA; (b–k) 3.0 μM HSA in the presence of 1.5, 3.0, 4.5, 6.0, 7.5, 9.0, 10.5, 12.0, 13.5, 15.0 μM LIG. The inset corresponds to the molecular structure of Z-ligustilide (LIG).

circulation is yet to be carried out. In an attempt to achieve a better understanding of the transport of LIG in human circulation, we report here in detail the binding characteristics of the LIG–HSA interaction as investigated by multiple spectroscopic probes. In addition, the effect of metal ions (e.g. Zn^{2+}, Cu^{2+}, Fe^{3+}, Co^{2+}, Ni^{2+}) on the binding of LIG–HSA complex was also studied.

2. Materials and methods

2.1. Materials

HSA (purity 96–99%, catalogue No. A1653) was purchased from Sigma–Aldrich Chemical Company (St. Louis, MO, USA)and dissolved in 0.05 M Tris–HCl buffer of pH 7.4 containing 0.10 M NaCl to form a 5.0×10^{-5} M stock solution, and then diluted to the required concentrations with the buffer. LIG was extracted and separated by a well-established procedure as described previously (Kuang et al., 2006; Zhao et al., 2014). The stock solution of LIG (5×10^{-3} M) was freshly prepared by dissolving LIG with methanol. The ultimate percentages of methanol in all solutions were below 1% (v/v). This low amount of methanol does not affect the structure of HSA (Chen et al., 2012). For CD spectra, the sodium phosphate buffer solution (0.02 M, pH 7.40) was selected according to the requirement of the apparatus. Other chemicals are of analytical reagent grade and ultra pure water is used throughout the study for preparation of solutions.

2.2. Methods

2.2.1. Fluorescence spectroscopy

Fluorescence measurements were carried out on RF-5301 PC spectrofluorimeter (Shimadzu, Japan) using a 1.0 cm path length quartz cuvette. The temperature of the sample was kept by Eyela water bath SB-11(Tokyo Rikakikai Co., Ltd, Tokyo, Japan).

A 3.0 ml solution containing 3.0 μM HSA was added to a 1.0 cm quartz cuvette, and then titrated by successive additions of 5.0 mM LIG solution. The titration was performed manually and mixed moderately after each injection for 5 min. The emission spectra of the HSA solutions (3.0 μM) in the absence and presence of LIG (0.0–15.0 μM with 1.5 μM intervals) were recorded at two temperatures (298 K and 310 K) in the wavelength range of 290–500 nm upon excitation at 280 nm. The widths of both the excitation and emission slits were set at 5 nm and 3 nm, respectively. An appropriate buffer was taken as the blank and subtracted from the experimental spectrum to correct background fluorescence.

Synchronous fluorescence spectra of HSA in the absence and presence of different amount of LIG were also recorded by scanning the excitation and emission monochromator simultaneously. The wavelength interval ($\Delta\lambda$) was fixed individually at 15 and 60 nm, at which the spectrum only showed the spectroscopic behaviour of tyrosine and tryptophan residues of HSA, respectively. The concentration of HSA was fixed at 3.0 μM while the LIG concentration was varied from 0.0 to 15.0 μM with 1.5 μM intervals.

2.2.2. UV–visible absorption spectroscopy

The UV–visible absorption spectra were recorded at room temperature on a UV-2450 spectrophotometer (Shimadzu, Japan) equipped with 0.5 cm quartz cells at wavelength ranging from 200 to 400 nm. The absorption spectra of HSA (3.0 μM), LIG (15.0 μM) and HSA–LIG complex whose molar ratio is 1:5 were recorded respectively.

2.2.3. CD spectroscopy

CD measurements of HSA in the absence and presence of LIG were carried out with a Chirascan spectrometer (Applied Photophysics Ltd., Leatherhead, Surrey, U.K.). The spectra were recorded from 200 to 260 nm with a scan speed of 50 nm/min and a bandwidth of 1 nm using 0.1 cm quartz cells. All the experiments were performed at room temperature. Nitrogen gas was utilized to purge the testing environment before and during the measurements. HSA concentration was kept at 3.0 μM, and molar ratios of LIG to HSA were varied as 0:1, 1:1, and 3:1. All observed CD spectra were corrected for buffer signal. The changes in the contents of different secondary structure were calculated using CDNN software equipped with the spectrometer.

3. Results and discussion

3.1. Fluorescence quenching mechanism of HSA by LIG

The fluorescence spectra of HSA for the successive addition of LIG are presented in Fig. 1. LIG exhibited native fluorescence at 400–500 nm. The spectra indicate that, with increasing LIG concentrations, the fluorescence intensity of HSA was decreased and the LIG peak increased in a regular manner (fluorescence spectra of HSA and LIG are in two different regions and do not overlap). Moreover, the blue shift from 336 nm to 333 nm in the fluorescence spectra corresponded to decreased polarity of the microenvironment after binding, which indicates that the chromophore of the protein was brought to more hydrophobic surroundings (Li, Chen, Wang, & Lu, 2013; Samari, Hemmateenejad, Shamsipur, Rashidi, & Samouei, 2012). Also, an isosbestic point can be seen, at which LIG–HSA has the same fluorescence intensity at about 399 nm. The isosbestic point is indicative of equilibrium between bound and free forms of the ligand (Iranfar, Rajabi, Salari, & Chamani, 2012). In other words, an isosbestic point was considered as a direct evidence for drug–protein complex formation.

3.2. The mechanism of quenching of HSA fluorescence by LIG

In order to understand the nature of the quenching mechanism of HSA in the presence of LIG, the well-known Stern–Volmer equation has been used for the analysis (Cahyana & Gordon, 2013; Skrt, Benedik, Podlipnik, & Ulrih, 2012).

$$\frac{F_0}{F} = 1 + K_q \tau_0 [Q] = 1 + K_{sv}[Q] \quad (1)$$

$$K_q = \frac{K_{sv}}{\tau_0} \quad (2)$$

where F_0 and F are the steady-state fluorescence intensities in the absence and presence of quencher, respectively, K_{sv} is the Stern–Volmer quenching constant, and $[Q]$ is the concentration of

quencher (LIG). τ_0 is the average lifetime of the protein without the quencher. Hence, Eq. (1) was applied to determine K_{sv} by linear regression of a plot of F_0/F against [Q]. Taking the average lifetime of molecular fluorescence (τ_0) as around 10^{-8} s (Anand, Jash, Boddepalli, Shrivastava, & Mukherjee, 2011), the quenching rate constant (K_q) could be obtained according to Eq. (2). Fig. S1 displays the Stern–Volmer plots of the quenching of HSA fluorescence by LIG at two different temperatures with a good linear relationship. The values of K_{sv} and K_q are given in Table 1. The values of K_q observed for HSA was of the order 10^{12} M^{-1} s^{-1}, which is 100-fold higher than the maximum value possible for diffusion controlled quenching of various kinds of quencher to biopolymer (2.0×10^{10} M^{-1} s^{-1}) (Chi & Liu, 2010). This observation suggests that there is a specific interaction between HSA and LIG, and the probable reason of fluorescence quenching is a static mechanism.

One additional method to distinguish static and dynamic quenching is by careful examination of the absorption spectra of the fluorophore. Collisional quenching only affects the excited states of the fluorophores, and thus, no changes in the absorption spectra are expected. In contrast, ground-state complex formation will frequently result in perturbation of the absorption spectrum of the fluorophore (Hu, Liu, & Xiao, 2009). As shown in Fig. S2, there is a strong absorption band at around 210 nm which is mainly due to the transition of $\pi \rightarrow \pi^*$ of HSA's characteristic polypeptide backbone structure C=O (Li, Abramavicius, Zhuang, & Mukamel, 2007; Zhong et al., 2009). Besides this, the absorption peak at about 278 nm can provide us with information about the three buried aromatic amino acids: Trp, Tyr, and Phe (Chen et al., 2012). Addition of LIG led to the decrease in absorbance of HSA at 210 nm, indicating disturbances to the microenvironment around the amide bonds in the protein. Meanwhile, the absorption peak at approximately 278 nm decreased (Fig. S2), which shows that more aromatic acid residues were buried into the hydrophobic environment. The conclusion agrees with the results from fluorescence spectra. The UV–visible absorption spectra of HSA (Fig. S2, curve a) and the difference absorption spectra between LIG–HSA complex and LIG (Fig. S2, curve c) could not be superposed. These results reconfirm that a ground-state complex is formed and the probable fluorescence quenching mechanism of HSA by LIG is a static quenching procedure.

3.3. Binding parameters

For the static quenching process, when small molecules bind independently to a set of equivalent sites on a biomacromolecule, the equilibrium between free and bound molecules is given by the following equation (Xiao, Cao, Wang, Yamamoto, & Wei, 2010):

$$\log_{10}\frac{F_0 - F}{F} = \log_{10} K_a + n\log_{10}[Q] \quad (3)$$

where F_0 and F are the fluorescence intensities in the absence and presence of the quencher, respectively, K_a is the binding constant, n is the number of binding sites per albumin molecule and [Q] is the concentration of quencher. Fig. 2 showed the plots of $\log_{10}(F_0 - F)/F$ versus $\log_{10}$[Q] for the LIG–HSA system at different temperatures, the calculated binding constants (K_a) and the number of binding sites (n) are presented in Table 1.

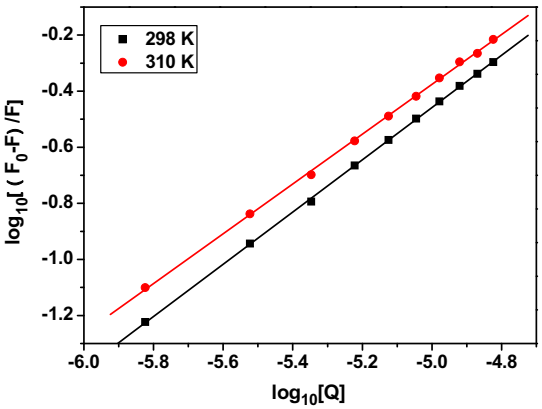

Fig. 2. Plots of $\log_{10}$ $(F_0 - F)/F$ against $\log_{10}$ [Q] for LIG quenching effect on HSA fluorescence at different temperatures.

The binding constants (K_a) between LIG and HSA were 1.59×10^4 M^{-1} (298 K) and 1.16×10^4 M^{-1} (310 K), respectively. The values of binding constant decreased with increasing the temperature, which may indicate forming an unstable complex, and the unstable complex would be partly decomposed with the rising temperature (Wang, Zhang, Zhou, & Xu, 2009). The values of n approximately to 1, which indicated that there exists a single binding site in HSA for LIG.

Generally speaking, the interaction forces between drugs and proteins include hydrogen bonds, van der Waals forces, electrostatic forces, and hydrophobic interaction forces. Thermodynamic parameters, free energy (ΔG), standard enthalpy (ΔH) and standard entropy (ΔS) can provide an insight into the binding mode (Ross & Subramanian, 1981). When temperature varies in a small range, the ΔH can be considered as a constant. Then through the binding constant K_a, thermodynamic parameters are evaluated using the following equations:

$$\Delta G = -RT \ln K_a \quad (4)$$

$$\ln\frac{K_{a2}}{K_{a1}} = \left[\frac{1}{T_1} - \frac{1}{T_2}\right]\frac{\Delta H}{R} \quad (5)$$

$$\Delta S = \frac{\Delta H - \Delta G}{T} \quad (6)$$

where K_a is binding constant at corresponding temperature and R is the gas constant 8.314 J mol^{-1} K^{-1}, and T is the absolute temperature. Values of ΔH, ΔS and ΔG obtained at two different temperatures using Eqs. (4)–(6) are listed in Table 1. ΔH for the binding reactions between LIG and HSA was −20.11 kJ mol^{-1}, and ΔS for the binding reactions between LIG and HSA was 12.96 J mol^{-1} K^{-1}. The favourable entropic contribution as reflected from the positive ΔS value obtained from LIG–HSA interaction can be attributed to several phenomena including hydrophobic interactions, and

Table 1
Stern–Volmer quenching constants (K_{sv}) and binding constants (K_a) and relative thermodynamic parameters of the system of LIG–HSA at different temperatures.

T (K)	Eq. (1)			Eq. (3)					
	10^{-4} K_{sv} (M^{-1})	10^{-12} K_q (M^{-1} s^{-1})	R[a]	10^{-4} K_a (M^{-1})	n	R[b]	ΔH (kJ mol^{-1})	ΔS (J mol^{-1} K^{-1})	ΔG (kJ mol^{-1})
298	3.36	3.36	0.9995	1.59	0.93	0.9999	−20.11	12.96	−23.97
310	3.99	3.99	0.9989	1.16	0.89	0.9983			−24.13

[a] R is the correlation coefficient of Eq. (1).
[b] R is the correlation coefficient of Eq. (3).

desolvation of the binding site, which involves the destruction of the ordered solvent layers surrounding the ligand and the protein binding site and removal of solvent molecules from the binding pocket (Olsson, Williams, Pitt, & Ladbury, 2008; Ross & Rekharsky, 1996). The role of hydrophobic interactions in the LIG–HSA complexation can be rationalized from the structure features of LIG, which possesses an isobenzofuranone connected by a butylidene side chain giving it a non-polar character. The involvement of ionic forces in the binding reaction between LIG and HSA is highly improbable due to a significantly higher value of ΔH obtained for this reaction as these forces are characterized by a $\Delta H \approx 0$ (Ross & Subramanian, 1981). In addition, absence of any ionisable group in LIG further rules out the participation of ionic forces in LIG–HSA interaction. A negative ΔH value obtained for LIG–HSA system can account for the involvement of hydrogen bonding and/or van der Waals forces (Ross & Rekharsky, 1996; Ross & Subramanian, 1981). Taking into consideration the possibility of several short-range interactions in LIG–HSA complexation, it would be inconceivable to assume the involvement of a single acting force in LIG–HSA interaction. Therefore, hydrophobic and van der Waals forces along with hydrogen bonds are believed to contributed collectively to the overall energetic of LIG–HSA interaction.

3.4. Energy transfer between LIG and HSA

According to fluorescence resonance energy transfer (FRET) theory, the parameters related to energy transfer can be calculated on the basis of equations as follows (Zaidi et al., 2013). The efficiency of energy transfer (E) can be calculated as:

$$E = 1 - \frac{F}{F_0} = \frac{R_0^6}{(R_0^6 + r^6)} \tag{7}$$

where E denotes the efficiency of energy transfer between the donor and acceptor, and r is the binding distance between donor and acceptor. R_0, the critical distance at which the transfer efficiency equals 50%, is given by the following equation:

$$R_0^6 = 8.79 \times 10^{-25} K^2 N^{-4} \Phi J \tag{8}$$

In Eq. (8) K^2 is the orientation factor to the donor and acceptor of dipoles, N is the refractive index of the medium, Φ is the fluorescence quantum yield of the donor, and J is the overlap integral of the fluorescence emission spectrum of the donor and the absorption spectrum of the acceptor, which could be calculated by Eq. (9):

$$J = \frac{\int_0^\infty F(\lambda)\varepsilon(\lambda)\lambda^4 d\lambda}{\int_0^\infty F(\lambda) d\lambda} \tag{9}$$

Here $F(\lambda)$ is the fluorescence intensity of the fluorescence donor at wavelength λ and, $\varepsilon(\lambda)$ is the extinction coefficient of the acceptor at λ. A significant overlap between the emission spectrum of HSA and LIG absorption spectrum was shown in Fig. 3, suggesting possibility of energy transfer between these molecules. It has been reported for HSA that $K^2 = 2/3$, $N = 1.336$, and $\Phi = 0.118$ (Lakowicz, 2006). According to the Eqs. (7)–(9), we could calculated that $J = 1.20 \times 10^{-14}$ cm^3 L mol^{-1}, $E = 0.085$, $R_0 = 2.53$ nm, and $r = 3.75$ nm. An r value is on the 2–8 nm scale, and $0.5R_0 < r < 1.5R_0$, indicating an existence of an interaction between LIG and HSA.

3.5. Conformational investigations

Circular dichroism (CD) spectroscopy is regarded as the best tool to observe the structure, conformation, and stability of protein in solution. As shown in Fig. 4, the CD spectra of the native HSA exhibits two negative bands in the far-UV region at 209 and 223 nm, which correspond to α-helical conformation of HSA. The rational elucidation is that the negative bands at 209 nm and

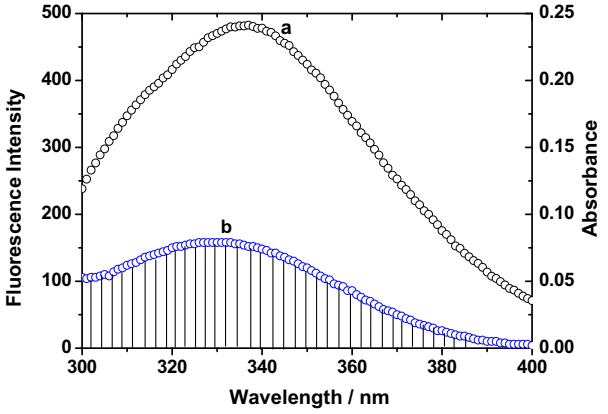

Fig. 3. The overlap of the UV–vis absorption of LIG with the fluorescence emission spectrum of HSA: (a) the fluorescence spectrum of HSA, [HSA] = 3.0 μM and (b) the UV–vis absorbance spectrum of LIG, [LIG] = 15.0 μM.

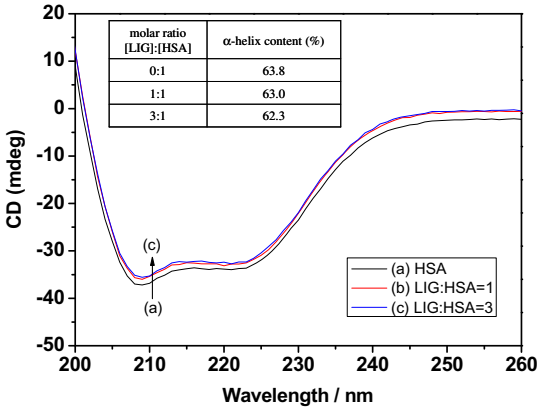

Fig. 4. Far UV-CD spectra of HSA in the presence of varying concentration of LIG in the range of 200–260 nm. (a) 3.0 μM HSA; (b) [LIG]: [HSA] = 1: 1; (c) [LIG]: [HSA] = 3: 1. Inset shows the α-helix structure content of HSA in the different concentration of LIG.

223 nm are both contributed by the $\pi \rightarrow \pi^*$ and the $n \rightarrow \pi^*$ transition for the peptide bond of α-helix (Kelly, Jess, & Price, 2005). The data compiled in the inset of Fig. 4 indicate the percentage of α-helix decreased slightly, from 63.8% in free HSA to 62.3% upon LIG binding. The observed slightly decrease in percent α-helix content might be induced by the formation of LIG–HSA complex. The results showed that the drug, LIG has less effect on the secondary structure of HSA. Therefore, HSA is a kind of the carrier protein which can safely carry LIG to reach the target tissues.

3.6. Effect of metal ions on the affinity of LIG for HSA

There are many metal ions in blood plasma that are involved in many biochemical processes. There is a wide variety of metal binding sites on albumin. HSA usually act as sequestration agent of metal ions and has a variety of metal sites with different specificities. The binding of metal ions, such as Cu^{2+}, Ni^{2+}, Zn^{2+}, Co^{2+} and other metal ions to serum albumin has been widely reported (Aime, Canton, Geninatti Crich, & Terreno, 2002; Liang et al., 2001; Sadler & Viles, 1996; Sun & Yee Szeto, 2003; Zhou et al., 1992). The phenomenon of HSA conformational changes caused by metal ions-HSA binding was observed in metal ion-HSA interaction process. And also many metal ions can form complexes with drug, thereby affecting the property of the drug. It is reasonable

Table 2
Binding parameters of LIG–HSA at 298 K in the presence of different metal ions obtained from fluorescence quenching experiment.

	HSA	HSA-Zn^{2+}	HSA-Cu^{2+}	HSA-Fe^{3+}	HSA-Co^{2+}	HSA-Ni^{2+}
K_a ($\times 10^4$ M^{-1})	1.59	0.88	1.32	0.76	1.27	0.50
n	0.93	0.88	0.91	0.86	0.90	0.82
R[a]	0.9999	0.9998	0.9998	0.9994	0.9998	0.9997

[a] R is the correlation coefficient.

to expect that metal ions affect the interaction of clinical drug with HSA in a ternary system of drug–protein–metal ion, and thus the distribution, pharmacological properties and metabolism of the drug in blood. Therefore, it is necessary to investigate the interactions of proteins and drugs in the presence of metal ions and such studies will be important in providing basic information on the pharmacological actions, biotransformation, and biodistribution of drugs.

In plasma, there are some metal ions that can participate in many vital actions and affect the reactions of the drugs with the plasma protein. So the effects of common metal ions (e.g. Zn^{2+}, Cu^{2+}, Fe^{3+}, Co^{2+}, Ni^{2+}) on binding constants of LIG–HSA complex were also investigated at 298 K. Fig. S3 showed the plots of $\log_{10}(F_0 - F)/F$ versus $\log_{10}[Q]$ for the LIG–HSA system in presence of metal ions. The values of binding constant and the number of binding sites acquired were listed in Table 2. The values of K_a for LIG–HSA system with Zn^{2+}, Cu^{2+}, Fe^{3+}, Co^{2+} and Ni^{2+} were 8.80×10^3, 1.32×10^4, 7.62×10^3, 1.27×10^4, and 4.96×10^3 M^{-1}, respectively. Compared with the K_a of LIG–HSA system without metal ions (1.59×10^4 M^{-1}), the existence of Zn^{2+}, Cu^{2+}, Fe^{3+}, Co^{2+} and Ni^{2+} decreased the binding constant between LIG and HSA, which resulted from certain competition among metal ions and LIG for HSA, and the formation of metal ions-HSA complexes was likely to affect the conformation of HSA and restrained the binding of LIG–HSA. The decrease in the binding constant value will improve the free concentrations of unbound drug, resulting in a shortening storage time of the drug in blood plasma together with an enhancement of the maximum effectiveness of the drug (He et al., 2005).

4. Conclusions

The present work reports the interaction of LIG from *Radix Angelica sinensis* to HSA. Results indicated that LIG binds to HSA with a moderate affinity. The quenching mechanism of fluorescence of HSA by LIG is a static process (with the formation of a HSA–LIG complex). The thermodynamic data suggested the involvement of van der Waals force, hydrophobic interaction, and hydrogen bonding in the complexation between LIG and HSA. Furthermore, the conformation of HSA was proved to be slightly disturbed upon the addition of LIG with a shrinkage of α-helix. We expect that this work contributes to better understanding of LIG with the serum albumin which is important for evaluation of the drug distribution and metabolic lifetime.

Acknowledgements

We greatly appreciate the support of the National Natural Science Foundation of China (21201105, 61171015, 21203103), Natural Science Foundation of Jiangsu Province (BK20131200), Natural Science Foundation of Jiangsu Higher Education Institutions of China (12KJB150019), Natural Science Foundation of Nantong City (BK2012012, BK2013051), and National Training Programs of Innovation and Entrepreneurship for Undergraduates (201310304018Z, 201410304044Z). This work is also sponsored by Qing Lan Project of Jiangsu Province and Innovation Found of Nantong University.

Appendix A. Supplementary data

Supplementary data associated with this article can be found, in the online version, at http://dx.doi.org/10.1016/j.foodchem.2014.11.041.

References

Aime, S., Canton, S., Geninatti Crich, S., & Terreno, E. (2002). ^1H and ^{17}O relaxometric investigations of the binding of Mn(II) ion to human serum albumin. *Magnetic Resonance in Chemistry, 40*, 41–48.
Anand, U., Jash, C., Boddepalli, R. K., Shrivastava, A., & Mukherjee, S. (2011). Exploring the mechanism of fluorescence quenching in proteins induced by tetracycline. *Journal of Physical Chemistry B, 115*, 6312–6320.
Cahyana, Y., & Gordon, M. H. (2013). Interaction of anthocyanins with human serum albumin: Influence of pH and chemical structure on binding. *Food Chemistry, 141*, 2278–2285.
Chen, T. T., Zhu, S. J., Lu, Y. P., Cao, H., Zhao, Y., Jiang, G. Q., et al. (2012). Probing the interaction of anti-cancer agent dihydromyricetin with human serum albumin: A typical method study. *Anti-Cancer Agents in Medical Chemistry, 12*, 919–928.
Chi, Z., & Liu, R. (2010). Phenotypic characterization of the binding of tetracycline to human serum albumin. *Biomacromolecules, 12*, 203–209.
Ghuman, J., Zunszain, P. A., Petitpas, I., Bhattacharya, A. A., Otagiri, M., & Curry, S. (2005). Structural basis of the drug-binding specificity of human serum albumin. *Journal of Molecular Biology, 353*, 38–52.
He, W., Li, Y., Xue, C., Hu, Z., Chen, X., & Sheng, F. (2005). Effect of Chinese medicine alpinetin on the structure of human serum albumin. *Bioorganic and Medicinal Chemistry, 13*, 1837–1845.
He, X. M., & Carter, D. C. (1992). Atomic structure and chemistry of human serum albumin. *Nature, 58*, 209–215.
Hu, Y. J., Liu, Y., & Xiao, X. H. (2009). Investigation of the interaction between Berberine and human serum albumin. *Biomacromolecules, 10*, 517–521.
Iranfar, H., Rajabi, O., Salari, R., & Chamani, J. (2012). Probing the interaction of human serum albumin with ciprofloxacin in the presence of silver nanoparticles of three sizes: Multispectroscopic and ξ potential investigation. *Journal of Physical Chemistry B, 116*, 1951–1964.
Kelly, S. M., Jess, T. J., & Price, N. C. (2005). How to study proteins by circular dichroism. *Biochimica et Biophysica Acta, 1751*, 119–139.
Kuang, X., Yao, Y., Du, J. R., Liu, Y. X., Wang, C. Y., & Qian, Z. M. (2006). Neuroprotective role of Z-ligustilide against forebrain ischemic injury in ICR mice. *Brain Research, 1102*, 145–153.
Lakowicz, J. R. (2006). *Principles of fluorescence spectroscopy*. New York: Plenum Press.
Li, Z. Y., Abramavicius, D., Zhuang, W., & Mukamel, S. (2007). Two dimensional electronic correlation spectroscopy of the nπ*and ππ* protein protein backbone transitions: A simulation study. *Chemical Physics, 341*, 29–36.
Li, X. R., Chen, D. J., Wang, G. K., & Lu, Y. (2013). Study of interaction between human serum albumin and three antioxidants: Ascorbic acid, α-tocopherol, and proanthocyanidins. *European Journal of Medical Chemistry, 70*, 22–36.
Liang, H., Huang, J., Tu, C. Q., Zhang, M., Zhou, Y. Q., & Shen, P. W. (2001). The subsequent effect of interaction between Co^{2+} and human serum albumin or bovine serum albumin. *Journal of Inorganic Biochemistry, 85*, 167–171.
Olsson, T. S. G., Williams, M. A., Pitt, W. R., & Ladbury, J. E. (2008). The thermodynamics of protein–ligand interaction and solvation: Insights for ligand design. *Journal of Molecular Biology, 384*, 1002–1017.
Ross, D. P., & Subramanian, S. (1981). Thermodynamics of protein association reactions: Forces contributing to stability. *Biochemistry, 20*, 3096–3102.
Ross, P. D., & Rekharsky, M. V. (1996). Thermodynamics of hydrogen bond and hydrophobic interactions in cyclodextrin complexes. *Biophysical Journal, 71*, 2144–2154.
Sadler, P. J., & Viles, J. H. (1996). ^1H and ^{113}Cd NMR investigations of Cd^{2+} and Zn^{2+} binding sites on serum albumin: Competition with Ca^{2+}, Ni^{2+}, Cu^{2+}, and Zn^{2+}. *Inorganic Chemistry, 35*, 4490–4496.
Samari, F., Hemmateenejad, B., Shamsipur, M., Rashidi, M., & Samouei, H. (2012). Affinity of two novel five-coordinated anticancer Pt(II) complexes to human and bovine serum albumins: A spectroscopic approach. *Inorganic Chemistry, 51*, 3454–3464.
Skrt, M., Benedik, E., Podlipnik, C., & Ulrih, N. P. (2012). Interactions of different polyphenols with bovine serum albumin using fluorescence quenching and molecular docking. *Food Chemistry, 135*, 2418–2424.
Sudlow, G., Birkett, D. J., & Wade, D. N. (1975). The characterization of two specific drug binding sites on human serum albumin. *Molecular Pharmacology, 11*, 824–832.

Sugio, S., Kashima, A., Mochizuki, S., Noda, M., & Kobayashi, K. (1999). Crystal structure of human serum albumin at 2.5 Å resolution. *Protein Engineering, 12*, 439–446.

Sun, H., & Yee Szeto, K. (2003). Binding of bismuth to serum proteins: Implication for targets of Bi(III) in blood plasma. *Journal of Inorganic Biochemistry, 94*, 114–120.

Varshney, A., Rehan, M., Subbarao, N., Rabbani, G., & Khan, R. H. (2011). Elimination of endogenous toxin, creatinine from blood plasma depends on albumin conformation: Site specific uremic toxicity & impaired drug binding. *PLoS One, 6*, e17230.

Wang, Y. Q., Zhang, H. M., Zhou, Q. H., & Xu, H. L. (2009). A study of the binding of colloidal Fe_3O_4 with bovine hemoglobin using optical spectroscopy. *Colloids and Surfaces A: Physicochemical and Engineering Aspects, 337*, 102–108.

Xiao, J. B., Cao, H., Wang, Y. F., Yamamoto, K., & Wei, X. L. (2010). Structure–affinity relationship of flavones on binding to serum albumins: Effect of hydroxyl groups on ring A. *Molecular Nutrition & Food Research, 54*, S253–S260.

Xiao, J. B., & Kai, G. Y. (2012). A review of dietary polyphenol–plasma protein interactions: Characterization, influence on the bioactivity, and structure–affinity relationship. *Critical Reviews in Food Science and Nutrition, 52*, 85–101.

Xiao, J. B. (2013). Polyphenol–plasma proteins interaction: Its nature, analytical techniques, and influence on bioactivities of polyphenols. *Current Drug Metabolism, 14*, 367–368.

Yin, J., Wang, C., Mody, A., Bao, L., Hung, S. H., Svoronos, S. A., et al. (2013). The effect of Z-ligustilide on the mobility of human glioblastoma T98G cells. *PLoS One, 8*, e66598.

Zaidi, N., Ahmad, E., Rehan, M., Rabbani, G., Ajmal, M. R., Zaidi, Y., et al. (2013). Biophysical insight into furosemide binding to human serum albumin: A study to unveil its impaired albumin binding in uremia. *Journal of Physical Chemsitry B, 117*, 2595–2604.

Zhao, L. X., Jiang, B. C., Wu, X. B., Cao, D. L., & Gao, Y. J. (2014). Ligustilide attenuates inflammatory pain via inhibition of NFκB-mediated chemokines production in spinal astrocytes. *European Journal of Neuroscience, 39*, 1391–1402.

Zhong, J., Song, L., Meng, J., Gao, B., Chu, W. S., Xu, H. Y., et al. (2009). Bio-nano interaction of proteins adsorbed on single-walled carbon nanotubes. *Carbon, 47*, 967–973.

Zhou, Y. Q., Hu, X. Y., Dou, C., Liu, H., Wang, S. Y., & Shen, P. W. (1992). Structural studies on metal-serum albumin. IV. The interaction of Zn(II), Cd(II) and Hg(II) with HSA and BSA. *Biophysical Chemistry, 42*, 201–211.